

Carbazole side-chained benzodithiophene based two-dimensional D-A conjugated photovoltaic polymers

Feng Li^{a,1}, Xin Song^{b,c,1}, Kaili Zhang^b, Bilal Shahid^c, Quanliang Wang^b, Liangmin Yu^d, Dangqiang Zhu^{c,*}, Mingliang Sun^{b,**}

^a Key Laboratory of Rubber-Plastics of Ministry of Education/Shandong Province, School of Polymer Science and Engineering, Qingdao University of Science & Technology, Qingdao, 266042, China

^b School of Materials Science and Engineering, Ocean University of China, Qingdao, 266100, China

^c CAS Key Laboratory of Bio-based Materials, Qingdao Institute of Bioenergy and Bioprocess Technology, Chinese Academy of Sciences, Qingdao, 266101, China

^d Key Laboratory of Marine Chemistry Theory and Technology, Ministry of Education, Ocean University of China, Qingdao, 266100, China



ARTICLE INFO

Keywords:

Carbazole
Side chain
Benzodithiophene
Polymer solar cells

ABSTRACT

In this work, one novel carbazole side chained benzodithiophene (BDT) monomer is designed and synthesized, and this new donor monomer based two D–A conjugated polymers with electron-withdrawing acceptor 4,7-di (4-(2-ethylhexyl)-2-thienyl)-5,6-difluoro-2,1,3-benzothiadiazole (DTffBT) (P5) and benzodithiophene-4,8-dione (BDD) (P7) are prepared. The polymers show 1.65–1.85 eV band gap, which is similar to the polymer with same backbone. The P5 based polymer solar cells show acceptable PCE around 8% and low energy loss around 0.7 eV, which is similar to the fluorene side-chained polymer. P7 based polymer shows 1 V open-circuit voltage in both fullerene based and fullerene-free polymer solar cells. Molecular conformations, photophysical/electrochemical properties and film morphology of the device active layer blend films were also systematically investigated to reveal the structure–property relationships. This work suggests that carbazole unit is a promising π -conjugated side chain group for BDT monomer to construct efficient two-dimensional (2D) D–A conjugated photovoltaic polymers.

1. Introduction

In the last two decades, the power conversion efficiency (PCE) of polymer solar cells has achieved 17% in tandem configuration [1] and 14% in single device structure [2]. Among all kinds of efficient polymer donor materials, benzodithiophene (BDT) based polymer is a star material due to the planar chemical structure, high mobility and easy modification. Lots of benzodithiophene backbone polymers, such as medium band-gap polymer PCE10 and wide band-gap polymers PBDB-T, J71 and etc., have been widely reported as donor for fullerene and non-fullerene-based PSCs [3]. Typically there are two main strategies to optimize the BDT based PSCs donor material. One is the main chain engineering which can mainly modulate the energy band gap and energy level of the materials, and the other is the side chain engineering which can mainly modulate the polymer donor solubility and device active layer morphology and etc. [3] Up to now, the high efficiency BDT materials are based on two dimensional (2D) structure which is

achieved by attaching conjugated units to BDT core as side chain [3]. The conjugated side chain can be alkylthienyl, benzothiophene, naphthyl and etc. [4–6] Yang and coworkers also reported about 1D-2D conjugated asymmetric benzodithiophene based high efficiency fullerene and fullerene-free polymer solar cells [7–9]. Due to the rigidity, high hole mobility and highly conjugated structures, recently, our group also introduced the fluorene unit as the conjugated side chain of benzodithiophene photovoltaic polymer and the PSCs devices showed low energy loss with acceptable PCE around 7% [10].

As we all know, the carbazole unit has also been widely used in organic electronic field such as the light emitting materials or hole transport materials in organic small molecule/polymer light emitting diodes [11,12]. Carbazole based conjugated materials also play a significant role in photovoltaic field, for example, the carbazole based small molecule or polymer can be used as perovskite solar cells transport materials [13], and carbazole are also widely used as electron-donating moiety to design D–A conjugated polymers due to their high hole

* Corresponding author.

** Corresponding author.

E-mail addresses: zhudq@qibebt.ac.cn (D. Zhu), milsun@ouc.edu.cn (M. Sun).

¹ Feng Li and Xin Song contributed equally to this work.

mobility and highly rigid conjugated structures [14]. Up till now, carbazole has been mainly used as main-chain unit to construct organic electronic materials. However, there are very few reports about carbazole side-chained polymer electronic materials, except the star material PVK [15].

In this work, one carbazole side-chained BDT monomer is designed and synthesized, and two D–A conjugated polymers P5 and P7 based on the novel electron-donating 2D BDT unit and electron-withdrawing acceptor 4,7-di(4-(2-ethylhexyl)-2-thienyl)-5,6-difluoro-2,1,3-benzothiadiazole (DTffBT) and benzodithiophene-4,8-dione (BDD) are prepared. The P5 based polymer solar cells show acceptable PCE around 8% and low energy loss around 0.7 eV, which is similar with fluorene side chained polymer [10]. P7 based polymer fullerene and fullerene-free PSC devices show 1 V high open-circuit voltage. This work suggests that carbazole moiety is a promising π -conjugated side chain group for BDT monomer to construct efficient 2D conjugated photovoltaic polymers.

2. Experimental procedures

2.1. Synthesis

2.1.1. 2-Bromo-9-(3-hexyldecyl)-9H-carbazole (2)

2-Bromo-9H-carbazole (9.0 g, 35.5 mmol) and potassium tert-butoxide (6.5 g, 44.3 mmol) are dissolved in 100 ml DMF at room temperature for 1 h, and then 1-bromo-3-hexyldecyl (16.7 g, 54.5 mmol) is added. The mixture is heated to 130 °C for 65 h. Then it was poured into water and extracted with petroleum ether. The organic phase was combined and dried over anhydrous Na_2SO_4 . Then the solvent was evaporated under vacuum and the residue was subjected to column chromatography on silica gel with petroleum ether. After removal of the solvent, the product (2) is obtained (yield: 89.3%).

$^1\text{H NMR}$ (600 MHz, CDCl_3) δ 8.05 (d, $J = 7.7$ Hz, 1H), 7.92 (d, $J = 8.2$ Hz, 1H), 7.51 (d, $J = 1.3$ Hz, 1H), 7.48–7.44 (m, 1H), 7.37 (d,

$J = 8.2$ Hz, 1H), 7.31 (dd, $J = 8.2, 1.5$ Hz, 1H), 7.23 (t, $J = 7.5$ Hz, 1H), 4.10 (d, $J = 7.5$ Hz, 2H), 2.15–2.03 (m, 1H), 1.39–1.18 (m, 27H), 0.86 (dt, $J = 11.7, 7.1$ Hz, 6H)

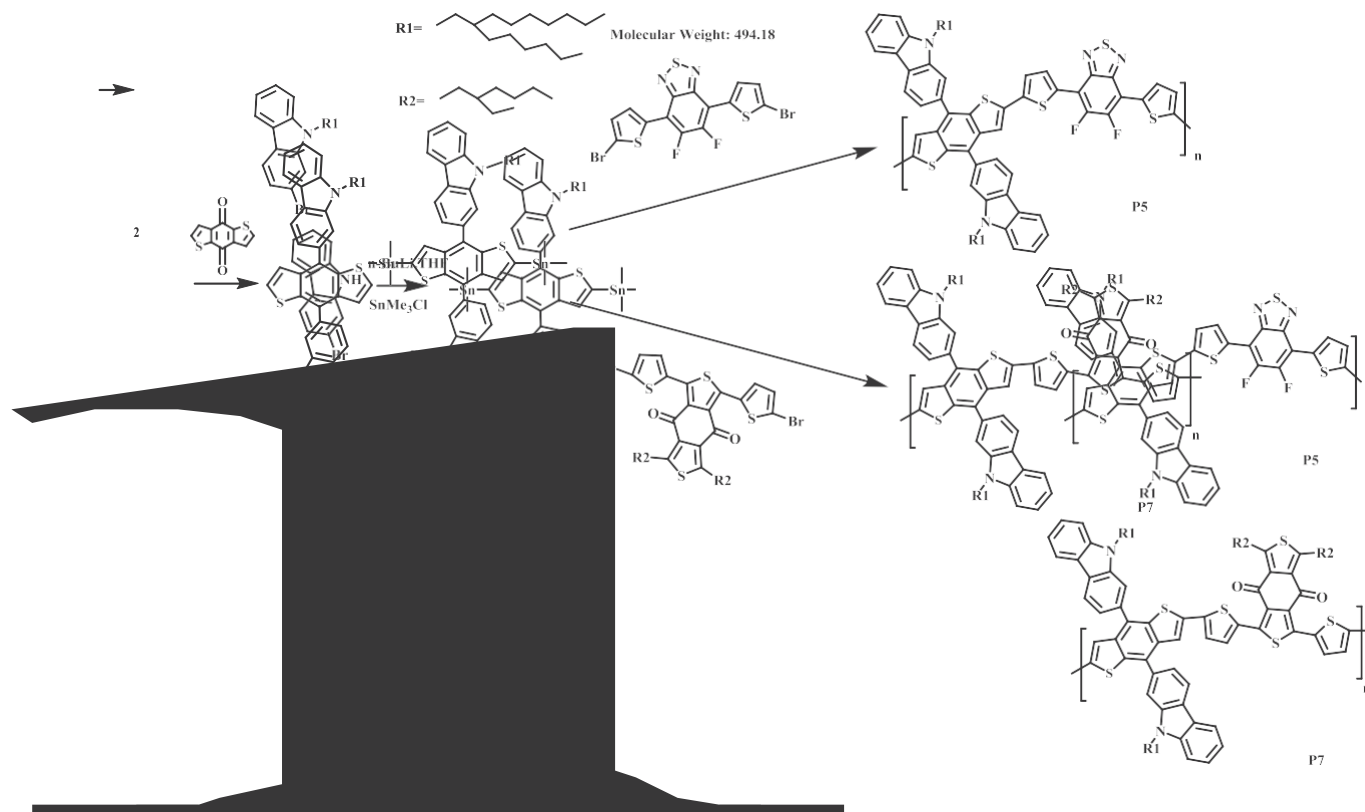
2.1.2. 4,8-Bis(9-(3-hexyldecyl)-9H-carbazol-2-yl)benzo[1,2-b:4,5-b']dithiophene (3)

Under the protection of argon, n-butyllithium (8.5 ml, 12.5 mmol) was added to (2) (4.9 g, 10.5 mmol) in dry THF (60.0 mL) at -78 °C and stirred for 2 h. Subsequently, dihydrobenzo[1,2-b:4,5-b']dithiophene-4,8-dione (1.1 g, 5.0 mmol) was added at -78 °C and stirred for 1 h. Then the mixture solution was warmed to room temperature and stirred overnight. SnCl_2 (11.3 g, 50.0 mmol) in 15% HCl (65.0 mL) was added, and the mixture was heated to 70 °C and stirred further for 6 h. 10 mL of ice water was added, and the mixture was extracted by petroleum ether. The extract was washed with water for three times and dried over anhydrous sodium sulfate. After removing the solvent by the rotary evaporator, the residue was purified by column chromatography on silica gel with petroleum ether as the eluent to afford 3 as light yellow solid (yield: 70.4%).

$^1\text{H NMR}$ (600 MHz, CDCl_3) δ 8.29 (d, $J = 7.9$ Hz, 2H), 8.19 (d, $J = 7.6$ Hz, 2H), 7.81 (s, 2H), 7.60 (d, $J = 7.9$ Hz, 2H), 7.51 (t, $J = 7.6$ Hz, 2H), 7.45 (dd, $J = 6.8, 3.1$ Hz, 4H), 7.41 (d, $J = 5.6$ Hz, 2H), 7.29 (t, $J = 7.4$ Hz, 2H), 4.21 (d, $J = 7.4$ Hz, 4H), 2.19 (d, $J = 5.8$ Hz, 2H), 1.44–1.17 (m, 54H), 0.86–0.81 (m, 12H).

2.1.3. 2,2'-(2,6-bis(trimethylstannyl)benzo[1,2-b:4,5-b']dithiophene-4,8-diyl)bis(9-(3-hexyldecyl)-9H-carbazole) (4)

Under the protection of argon, n-butyllithium (2.2 ml, 3.6 mmol) was added to (3) (1.4 g, 1.4 mmol) in dry THF (40.0 mL) at -78 °C for 1 h. Then the mixture solution was warmed to room temperature and stirred for 1 h. Then SnMe_3Cl (4.8 ml, 4.8 mmol) was added at -78 °C. The mixture was stirred overnight. 10 mL of ice water was added, and the mixture was extracted by petroleum ether. After the solvent was removed, the raw product was subjected to column chromatography on



Scheme 1. Synthetic route of P5 and P7 polymer.

Table 1
Basic properties of P5 and P7.

Polymer	M_n (kDa)	λ_{\max}^a nm	λ_{onset}^a nm	λ_{\max}^b nm	λ_{onset}^b nm	E_g^{optc} (eV)	HOMO ^{CV} (eV)	LUMO ^d (eV)
P5	20.4	600	725	620	750	1.65	-5.40	-3.75
P7	18.7	550	650	560	670	1.85	-5.47	-3.62

^a In *o*-DCB solution.

^b In pure film drop-cast from *o*-DCB solution.

^c Calculated from $E_g^{\text{opt}} = 1240/\lambda_{\text{onset}}$.

^d Obtained from $E_{\text{LUMO}} = E_g^{\text{opt}} + E_{\text{HOMO}}$.

silica gel with petroleum ether/CH₂Cl₂, and purified by recrystallization from acetone, and a light yellow solid (4) was obtained (yield: 76.6%). MS (ESI): 1296.

¹H NMR (600 MHz, CDCl₃) δ 8.30 (d, $J = 7.9$ Hz, 2H), 8.18 (d, $J = 7.6$ Hz, 2H), 7.83 (s, 2H), 7.62 (dd, $J = 7.8, 1.0$ Hz, 2H), 7.57–7.47 (m, 4H), 7.45 (d, $J = 8.1$ Hz, 2H), 7.28 (d, $J = 7.4$ Hz, 2H), 4.21 (s, 4H), 2.23 (s, 2H), 1.53–1.00 (m, 54H), 0.81 (dt, $J = 13.7, 7.1$ Hz, 12H), 0.61–0.09 (m, 18H).

¹³C NMR (151 MHz, CDCl₃) δ 142.95, 142.01, 141.58, 141.11, 137.45, 137.24, 131.01, 129.79, 125.75, 122.71, 122.47, 120.59, 120.49, 120.37, 118.93, 110.13, 109.08, 48.01, 38.07, 32.13, 31.85, 31.78, 29.95, 29.63, 29.49, 29.18, 26.75, 22.63, 22.54, 14.11, 14.09, 1.03, 0.00, -8.40.

2.1.4. Synthesis of P5 and P7 polymers

In a 25 mL flask, 4 (129.5 mg, 0.1 mmol) and 2BrDTff BT (49.4 mg, 0.1 mmol) or 2BrBDD (76.0 mg, 0.1 mmol), Pd₂(dba)₃ (1.8 mg), and tri(*o*-tolyl)phosphine (3.6 mg) were added under argon protection. After the addition of dry toluene (10.0 mL), the mixture was heated to 110 °C for 24 h. After cooling to room temperature, the mixture was poured into methanol. The precipitate was collected and filtered into a Soxhlet funnel successively with methanol, acetone, and hexane. The residue was collected and dried overnight under vacuum to afford polymers.

2.2. Materials characterization methods

¹H NMR and ¹³C NMR spectra of intermediates were collected on a Bruker AVANCE-III 600 Spectrometer at 298 K as solutions in CDCl₃. Gel permeation chromatography (GPC) was performed with THF as eluent and polystyrene was used as the standard. UV–vis absorption spectra were measured from a Hitachi U-4100 spectrophotometer with dilute solutions and solid state films of the polymers. Cyclic

voltammetry (CV) measurements were performed on a CHI660D electrochemical workstation, equipped with a three-electrode cell consisting of a platinum working electrode, a saturated calomel electrode (SCE) as reference electrode and a platinum wire counter electrode. CV measurements were carried out in anhydrous acetonitrile containing 0.1 M n-Bu₄NPF₆ as a supporting electrolyte under an argon atmosphere at a scan rate of 100 mV s⁻¹ assuming that the absolute energy level of Fc/Fc⁺ was -4.80 eV. Thin films were deposited from *o*-DCB solution onto the working electrodes. Density functional theory (DFT) calculations were confirmed by the Gaussian 09 program at the B3LYP/6-31G(d,p) level. Transmission electron microscopy (TEM) images were obtained by using a HITACHI H-7650 electron microscope with an acceleration voltage of 100 kV.

2.3. Device fabrication and evaluations

Photovoltaic devices were fabricated with a conventional device structure of ITO/PEDOT:PSS/polymer: PC₇₁BM(or ITIC)/Ca/Al. The patterned ITO glass (sheet resistance = 15 Ω /square) was pre-cleaned in an ultrasonic bath of acetone and isopropyl alcohol and treated in an ultraviolet-ozone chamber (PREEN II-862) for 6 min. Then a thin layer (about 30 nm) of PEDOT:PSS was spin-coated onto the ITO glass at 4000 rpm and baked at 150 °C for 15 min. Solutions of polymer/PC₇₁BM (ITIC) in *o*-DCB (25 mg/mL, total concentration) were stirred overnight and warmed to 50 °C for 30 min before spin-coating on the PEDOT:PSS layer to form the active layer about 100–120 nm. The thickness of the active layer was measured using a Veeco Dektak 150 profilometer. Finally, Ca (30 nm) and Al (100 nm) metal electrode was thermally evaporated under about 4×10^{-4} Pa and the device area was 0.1 cm² defined by shadow mask. The current density–voltage (J - V) characteristics were recorded with a Keithley 2400 source measurement unit under simulated 100 mW cm⁻² irradiation from a Newport solar simulator.

3. Result and discussion

3.1. Synthesis and characterization

The detailed synthetic route of the monomers and polymers is shown in Scheme 1. The carbazole-substituted BDT monomer was designed as electron-donating moiety (D), and DTffBT and BDD were selected as two electron-withdrawing acceptor moieties (A). The molecular structure of the intermediates was confirmed by ¹H NMR and ¹³C NMR spectroscopy. These two polymers P5 and P7 were prepared by Stille polymerization in the presence of Pd₂(dba)₃ and P(*o*-tolyl)₃ as catalyst and ligand, respectively. The polymers showed good solubility in common solvents such as chloroform, toluene and chlorobenzene (CB) at room temperature. The number average molecular weight (M_n) of both polymers was measured by gel permeation chromatography (GPC) analysis, using polystyrene as the reference and THF (40 °C) as the eluent. The M_n of the polymers P5 and P7 were estimated to be 20.4 and 18.7 kDa, respectively, as shown in Table 1.

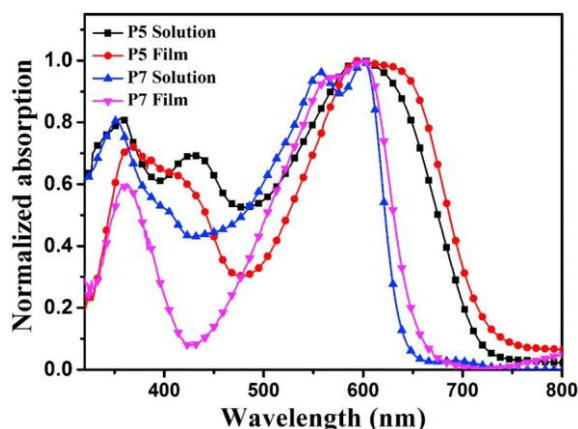


Fig. 1. UV–vis absorption spectra of P5 and P7 in dilute *o*-DCB solutions and thin films.

3.2. Optical and electrochemical properties

The normalized absorption spectra of polymers in both dilute ortho dichlorobenzene (*o*-DCB) solution and thin film at ambient temperature are shown in Fig. 1, and the corresponding absorption data are summarized in Table 1. As shown in Fig. 1, the polymer P5 (P7) shows broad absorption from 300 to 750 (670) nm, covering the whole visible spectrum. The absorption band region from 500 to 750 (670) nm originated from the intra-molecular charge transfer (ICT) process from the donor segments (BDT) to the acceptor segments (DTffBT or BDD), and the other minor absorption bands at about 350–500 nm is attributed to π - π^* transition of the donor units.

3.3. Electrochemical properties

The oxidation potentials of the polymers were determined by cyclic voltammetry (CV) with the polymer coated on glassy carbon electrodes. In order to obtain the oxidation potential of the polymers, the reference electrode was calibrated using ferrocene/ferrocenium (Fc/Fc⁺), which had a redox potential with an absolute energy level of 0.40 eV in a vacuum. The CV curves of polymers are shown in Fig. 2(a). The HOMO energy levels were calculated from their onset oxidation potential (ϕ_{ox}) according to the empirical equation $HOMO = -(\phi_{ox} + 4.80-0.40)$ (eV). The LUMO energy levels were calculated from the E_g^{opt} and HOMO level. The HOMO/LUMO energy levels of polymers P5 and P7 were calculated to be -5.40 eV/ -3.75 eV, and -5.47 eV/ -3.62 eV, respectively, and the relevant data are summarized in Table 1. The deep

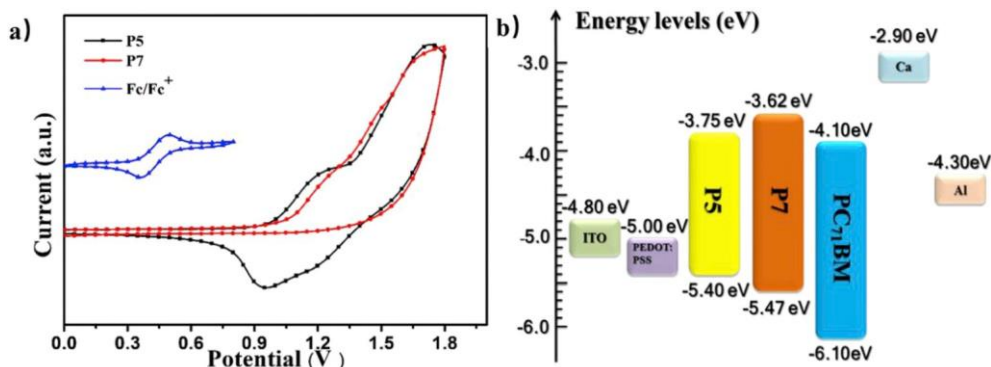


Fig. 2. (a) Cyclic voltammograms of polymers; (b) Energy level diagrams of the materials in this work.

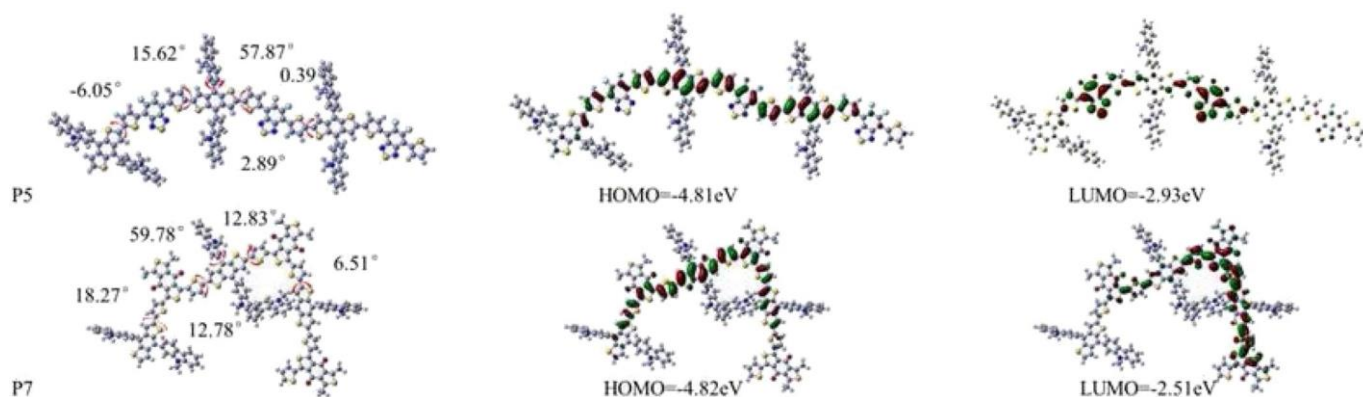


Fig. 3. Theoretically calculated molecular conformations, corresponding torsion angles and distributions of frontier energy levels of two polymers. Long alkyl chains were replaced by methyl groups. Gray: carbon (C); blue: nitrogen (N); red: oxygen (O) and yellow: sulfur (S). (For interpretation of the references to colour in this figure legend, the reader is referred to the Web version of this article.)

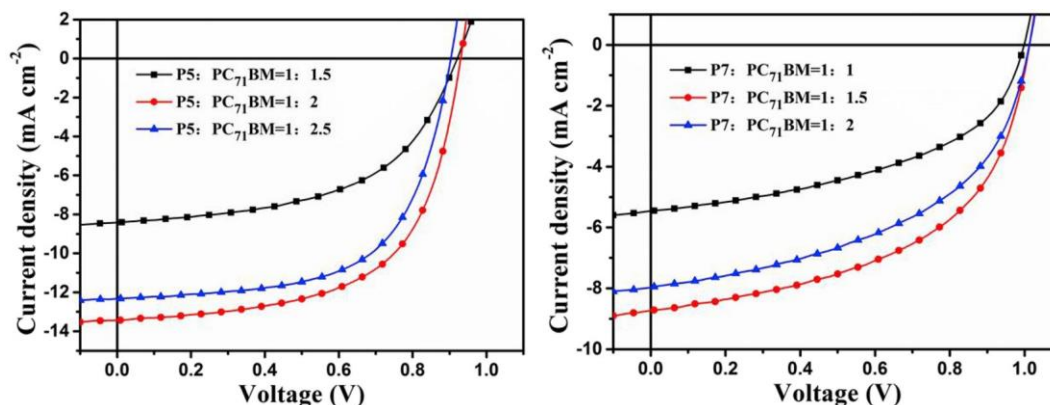


Fig. 4. *J*-*V* curves of polymer/PC₇₁BM solar cells under different weight ratio.

Table 2
Photovoltaic performance of PSCs devices based on P5 and P7/PC₇₁BM.

Polymer/ Acceptor	w/w	V _{oc} (V)	J _{sc} (mA cm ⁻²)	FF	PCE (%) ^a
P5/PC ₇₁ BM	1:1.5	0.92	8.53	0.535	4.18 (4.03 ± 0.09)
P5/PC ₇₁ BM	1:2	0.91	13.53	0.632	7.79 (7.57 ± 0.13)
P5/PC ₇₁ BM	1:2.5	0.90	12.27	0.536	6.87 (6.75 ± 0.10)
P7/PC ₇₁ BM	1:1	1.00	5.43	0.481	2.58 (2.47 ± 0.08)
P7/PC ₇₁ BM	1:1.5	1.01	8.62	0.524	4.56 (4.49 ± 0.06)
P7/PC ₇₁ BM	1:2	1.01	7.92	0.495	3.96 (3.77 ± 0.11)

^a The data were based on more than 10 devices and were provided in “highest (average)” format.

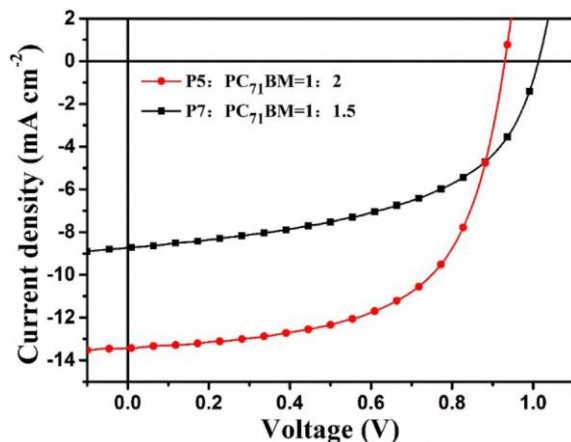


Fig. 5. J - V curves of polymer/PC₇₁BM solar cells under optimal weight ratio.

Table 3
Photovoltaic performance of PSCs devices based on P5 and P7/ITIC.

Polymer/ Acceptor	w/w	V _{oc} (V)	J _{sc} (mA cm ⁻²)	FF	PCE (%) ^a
P5/ITIC	1:1.5	0.99	11.61	0.357	4.10 (4.01 ± 0.07)
P5/ITIC	1:2	0.99	11.86	0.373	4.39 (4.33 ± 0.05)
P5/ITIC	1:2.5	0.97	11.39	0.335	3.70 (3.69 ± 0.01)
P7/ITIC	1:1	1.04	7.21	0.405	3.04 (2.97 ± 0.07)
P7/ITIC	1:1.5	1.01	9.74	0.487	4.79 (4.73 ± 0.05)
P7/ITIC	1:2	1.01	9.73	0.479	4.71 (4.67 ± 0.05)

^a The data were based on more than 10 devices and were provided in “highest (average)” format.

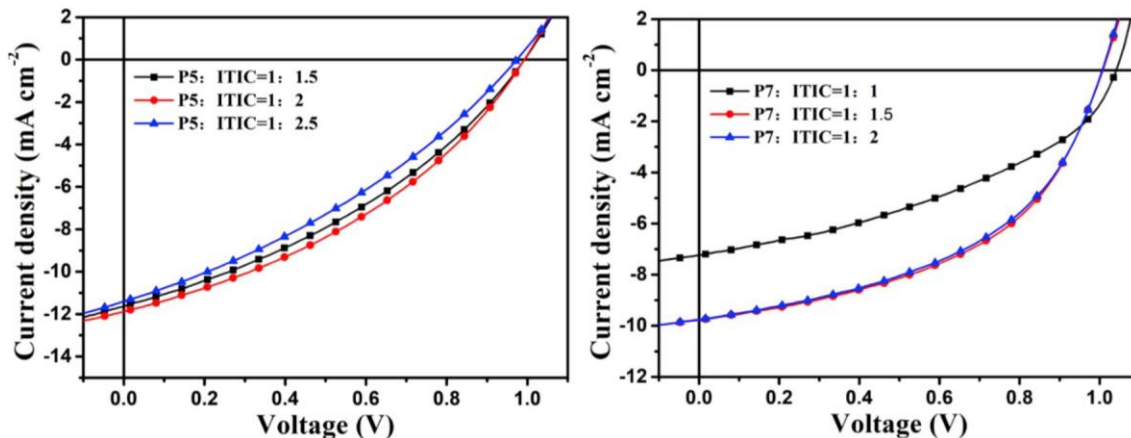


Fig. 6. J - V curves of polymer/ITIC solar cells under different weight ratio.

HOMO energy level of P7 would help to obtain a high V_{oc} in polymer solar cells.

3.4. Molecular conformational study

To further understand the influence of carbazole unit in BDT on the polymer backbone conformations, quantum chemical calculations (based on density functional theory, B3LYP/6-31G) were performed for three repeat units of two polymers. The alkyl chains in BDT and BDD units were replaced by methyl group to reduce the calculation time. From Fig. 3 we can see that the bulky carbazole units in BDT produce a large dihedral angle over 57° for two polymers. These highly twisting side groups are beneficial to improve the solubility of polymers and may induce decreased π -orbital overlap between side groups and polymer backbones. Compared with P7, the P5 polymer exhibits favorable planarity along polymer backbone, which could benefit the charge transport in PSCs active layer. From the distributions of electron density, both polymers show a delocalized HOMO which is distributed over both the donor and acceptor parts of D-A polymer. However, the LUMO energy levels are more localized on the acceptor units. Moreover, we can see from Fig. 3 that polymers P5 and P7 have comparable HOMO levels, but polymer P5 exhibits deeper LUMO levels, which is consistent with the results from CV measurement.

3.5. Photovoltaic properties

Single BHJ-PSCs were fabricated with a configuration of indium tin oxide (ITO)/poly(3,4-ethylenedioxythiophene)polystyrenesulfonate (PEDOT:PSS)/P5 or P7:PC₇₁BM/Ca/Al. The energy levels of the materials used in the devices are shown in Fig. 2(b). The donor-acceptor weight ratio was screened. The current density-voltage (J - V) curves at different D/A ratios under AM 1.5G (100 mW cm⁻²) illumination are shown in Fig. 4, and the device parameters are summarized in Table 2. As Table 2 shows, the optimal donor-acceptor weight ratio of P5/PC₇₁BM is 1:2, with PCE up to 7.79% and V_{oc} = 0.91 V, J_{sc} = 13.53 mA cm⁻², and FF = 0.632. For the devices based on polymer P7, the optimal donor-acceptor weight ratio is proved to be 1:1.5, with PCE of 4.56% and V_{oc} = 1.01 V, J_{sc} = 8.62 mA cm⁻², and FF = 0.524. The J - V curves under optimal weight ratio are displayed in Fig. 5. Notably, P5 based PSCs devices exhibit higher short-circuit current densities and PCE, while devices based on P7 exhibit significantly enhanced open-circuit voltage around 1.0 V. This should be attributed to its deep HOMO energy levels. To further optimize the solar cells performances, ITIC acceptor based devices were also systematically investigated. The detailed device performance is summarized in Table 3, and the J - V curves are shown in Figs. 6 and 7. Unfortunately, they do not show noticeable positive improvement.

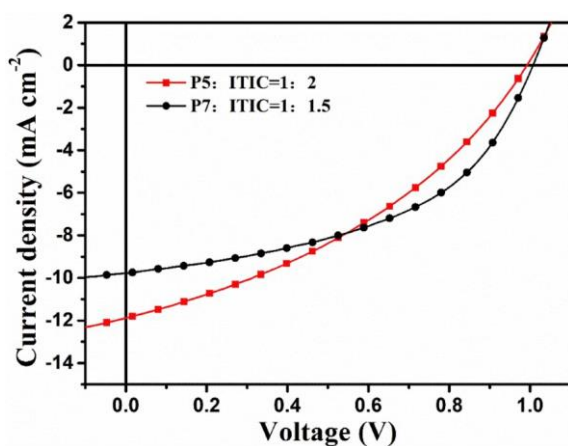


Fig. 7. J - V curves of polymer/ITIC solar cells under optimal weight ratio.

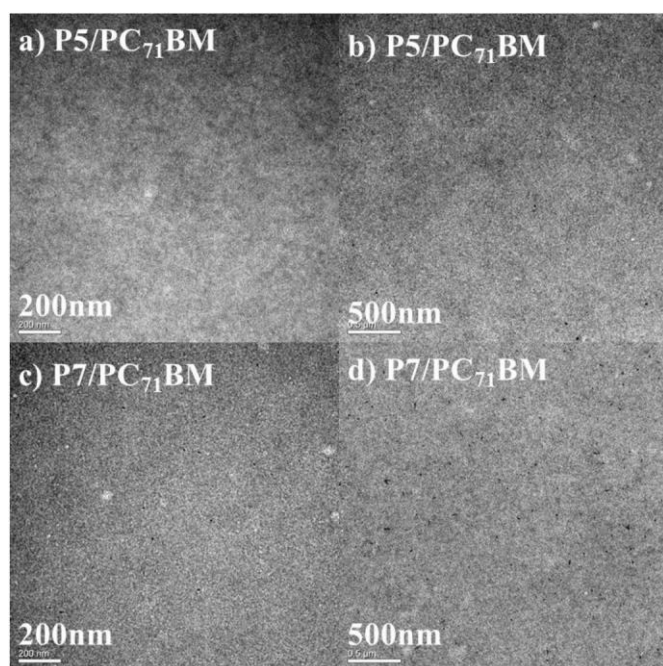


Fig. 8. TEM of P5/PC₇₁BM (1:2, w/w) and P7/PC₇₁BM (1:1.5, w/w) films.

3.6. BHJ morphology properties

Considering that the photovoltaic performance has a close correlation with the BHJ morphological properties, transmission electron microscope (TEM) measurements were applied to the active layer blends to study the difference of photovoltaic performance of DTffBT and BDD based polymers. The TEM images of P5/PC₇₁BM (1:2, w/w) and P7/PC₇₁BM blend films (1:1.5, w/w) are shown in Fig. 8. One can observe that both blends reveal morphological properties with similar polymer aggregations. The P5 based blend show more nanoscale phase separation which is beneficial for exciton diffusion to the donor/acceptor interface, charge separation and transport.

4. Conclusion

In this work, one novel carbazole side-chained BDT monomer is designed and synthesized and two D-A conjugated polymers based on this novel monomer and electron-withdrawing acceptor DTffBT (P5) BDD (P7) are prepared. The P5 based PSCs devices show moderate PCE around 8% and low energy loss around 0.7 eV, which is similar with fluorene side chained polymer. P7 based fullerene and fullerene-free PSC devices show high open-circuit voltage (over 1 V). This work suggests that the carbazole unit is a promising side chain group for 2D BDT photovoltaic polymers.

Acknowledgements

The authors are deeply grateful to Fundamental Research Funds for the Central Universities (201822002), Natural Science Foundation of Shandong Province (ZR2018MEM023) and National Natural Science Foundation of China (U1806223).

References

- [1] Meng L, Zhang Y, Wan X, Li C, Zhang X, Wang Y, Ke X, Xiao Z, Ding L, Xia R, Yip H, Cao Y, Chen Y. Organic and solution-processed tandem solar cells with 17.3% efficiency. *Science* 2018;361:1094–8.
- [2] Zhao W, Li S, Yao H, Zhang S, Zhang Y, Yang B, Hou J. Molecular optimization enables over 13% efficiency in organic solar cells. *J Am Chem Soc* 2017;139:7148–51.
- [3] Yao H, Ye L, Zhang H, Li S, Zhang S, Hou J. Molecular design of benzodithiophene-based organic photovoltaic materials. *Chem Rev* 2016;116:7397–457.
- [4] Huo L, Zhang S, Guo X, Xu F, Li Y, Hou J. Replacing alkoxy groups with alkylthienyl groups: a feasible approach to improve the properties of photovoltaic polymers. *Angew Chem Int Ed* 2011;50:9697–702.
- [5] Wang J, Xiao M, Chen W, Qiu M, Du Z, Zhu W, Wen S, Wang N, Yang R. Extending π -conjugation system with benzene: an effective method to improve the properties of benzodithiophene-based polymer for highly efficient organic solar cells. *Macromolecules* 2014;47:7823–30.
- [6] Ding D, Wang J, Du Z, Li F, Chen W, Liu F, Li H, Sun M, Yang R. A novel naphthyl side-chained benzodithiophene polymer for efficient photovoltaic cells with a high fill factor of 75%. *J Mater Chem A* 2017;5:10430–6.
- [7] Liu D, Zhu Q, Gu C, Wang J, Qiu M, Chen W, Bao X, Sun M, Yang R. High performance photovoltaic polymers employing symmetry-breaking building blocks. *Adv Mater* 2016;28:8490–8.
- [8] Liu Z, Liu D, Zhang K, Zhu T, Zhong Y, Li F, Li Y, Sun M, Yang R. Efficient fullerene-free solar cells with wide optical band gap polymers based on fluorinated benzotriazole and asymmetric benzodithiophene. *J Mater Chem A* 2017;5:21650–7.
- [9] Zhu T, Liu D, Zhang K, Li Y, Liu Z, Gao X, Bao X, Sun M, Yang R. Rational design of asymmetric benzodithiophene based photovoltaic polymers for efficient solar cells. *J Mater Chem A* 2018;6:948–56.
- [10] Song X, Zhang Y, Li Y, Li F, Bao X, Ding D, Sun M, Yang R. Fluorene side-chained benzodithiophene polymers for low energy loss solar cells. *Macromolecules* 2017;50:6880–7.
- [11] Jia Y, Zhang Y, Fan S, Wu S, Zhao X, Wang S, Li X. A novel bipolar carbazole/phenanthroimidazole derivative for high efficiency nonpopped deep-blue organic light-emitting diodes. *Org Electron* 2019;64:259–65.
- [12] Liu R, Xiong Y, Zeng W, Wu Z, Du B, Yang W, Sun M, Cao Y. Extremely color-stable blue light-emitting based on alternating 2,7-Fluorene/3,9-Carbazole-copolymer. *Macromol Chem Phys* 2007;208:1503–9.
- [13] Liu X, Ding X, Ren Y, Yang Y, Ding Y, Liu X, Alsaedi A, Hayat T, Yao J, Dai S. A star-shaped carbazole-based hole-transporting material with triphenylamine side arms for perovskite solar cells. *J Mater Chem C* 2018;6:12912–8.
- [14] Koutsoubelitis A, Seintis K, Tsikritzis D, Oriou J, Brochon C, Cloutet E, Hadziioannou G, Vasilopoulou M, Kennou S, Fakis M, Palilis L. Photophysics, electronic structure and solar cell performance of a donor-acceptor poly(N-dodecyl-2,7-carbazole-alt-benzothiadiazole) copolymer. *Org Electron* 2018;59:202–12.
- [15] Wang L, Chen T, Lin Q, Shen H, Wang A, Wang H, Li C, Li L. High-performance azure blue quantum dot light-emitting diodes via doping PVK in emitting layer. *Org Electron* 2016;37:280–6.